INVITED PAPER *Joint Special Section on Opto-electronics and Communications for Future Optical Network*

Ultra Fast Response AC-Coupled Burst-Mode Receiver with High Sensitivity and Wide Dynamic Range for 10G-EPON System

Kazutaka HARA[†a)], **Shunji KIMURA**[†], **Hirotaka NAKAMURA**[†], ***Members***,
Naoto YOSHIMOTO[†], ***Senior Member***, ***and*** **Hisaya HADAMA**[†], ***Member***

SUMMARY A 10-Gbit/s-class ac-coupled average-detection-type burst-mode receiver (B-Rx) with an ultra fast response and a high tolerance to the long consecutive identical digits has been developed. Key features of the circuit design are the baseline-wander common-mode rejection technique and the inverted distortion technique adopted in the limiting amplifier to cope with both the fast response and the high tolerance. Our B-Rx with newly developed limiting amplifier IC achieved a settling time of less than 150 ns, a sensitivity of −29.8 dBm, and a dynamic range of 23.8 dB with a $2^{31} - 1$ pseudo random bit sequences. Moreover, we also describe several potential B-Rx applications. We achieved better performance by applying the proposed systems to our B-Rx.

key words: *10G class access network, burst-mode receiver, passive optical network, transient-phenomena cancellation*

1. Introduction

Data traffic for broadband access networks providing large capacity content has been increasing exponentially over recent decades. Passive optical network (PON) systems have made it possible to realize economical fiber-to-the-home services. In PON systems, as shown in Fig. 1, several optical network units (ONUs) share one optical line terminal (OLT) through an optical fiber and a $1 : N$ optical splitter. An OLT broadcasts downstream data in a continuous mode. In contrast, upstream traffic is managed by using time division multiple access (TDMA) technology according to the grant signals from the OLT to avoid any overlap between burst data in the primary fiber. These burst-mode data have various optical power levels because of the different distances between the ONUs and the OLT, and arbitrary phase to each ONU.

Recently, the standardization of 10G-EPON and NG-PON systems has been actively discussed with a view to realizing PON systems offering even higher speeds [1]–[3]. These 10-Gbit/s class PON systems may provide various services such as IP-TV, Video on Demand (VOD), and promote an increase in the number of HD-TV-equipped homes, and wireless mobile backhaul. The most significant technical issue as regards 10G-bit/s class PON systems is the establishment of a 10-Gbit/s-class burst-mode transmitter (B-Tx) [4], [5] and a burst-mode receiver (B-Rx) [6]–[9]. In particular, the B-Rx should have a faster response to improve the upstream transmission efficiency, and a higher tolerance to long consecutive identical digits (CID) to guarantee error-free operation. The B-Rx has two circuit designs, namely the dc- and the ac-coupled B-Rx. The next section provides a detailed comparison of these circuits. We focused on an ac-coupled B-Rx as a cost-effective solution offering higher interoperability with a simple interface. However, an ac-coupled B-Rx is characterized by a trade off between a shorter ac-coupling time-constant or an increase in the average detector (AD) speed and the tolerance of CID. To overcome this problem, we have proposed the baseline-wander common-mode rejection (BLW-CMR) technique and the inverted distortion technique to cancel out the effect of ac-coupling and to shorten the AD time constant.

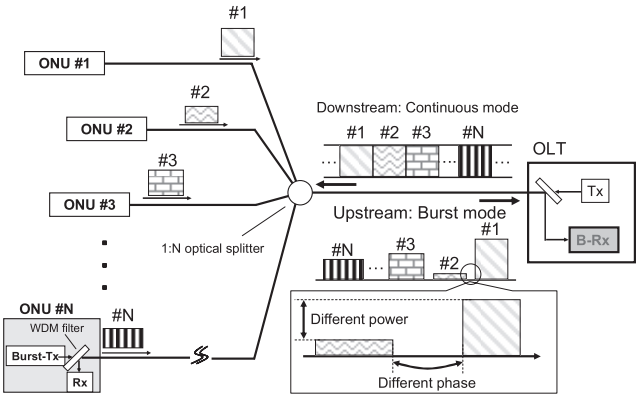

Fig. 1 PON system and data format.

In this work, we newly design the AD time constant of our B-Rx based on the ac-coupled configuration, and evaluate its receiver performance. Moreover, we suggest several B-Rx applications for optical access networks. First we describe a dual-rate PON system application that can provide existing services and 10-Gbit/s class services on the same optical distribution network. Second, we attempt to extend transmission with a PON system to over 20 km without using an optical amplifier, thus showing that this B-Rx is highly suitable for all types of networks.

2. Circuit Design

2.1 Data Format and Design Concept of the B-Rx

Generally speaking, there are three types of signal format

Manuscript received January 4, 2011.
Manuscript revised March 25, 2011.

[†]The authors are with NTT Access Network Service Systems Laboratories, NTT Corporation, Yokosuka-shi, 239-0847 Japan.
a) E-mail: hara.kazutaka@lab.ntt.co.jp

DOI: 10.1587/transcom.E94.B.1845

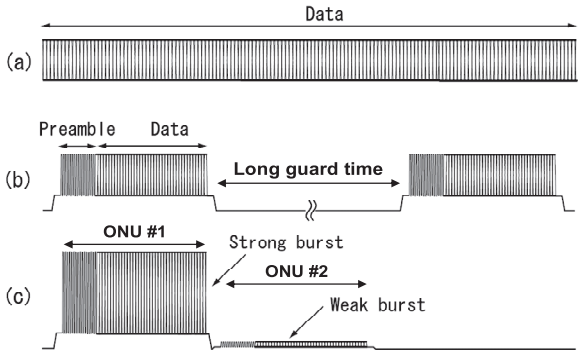

Fig. 2 Examples of three data formats. (a): Continuous-mode data. (b) Isolated pattern: Burst-mode data. (c) Fulfilled pattern: Burst-mode data with different amplitude.

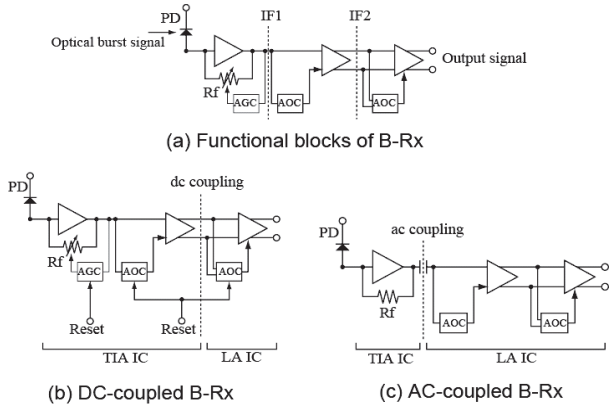

Fig. 3 Conventional configuration of B-Rxs. (a): Functional blocks of B-Rx (b): dc-coupled B-Rx (c): ac-coupled B-Rx.

in digital communication systems as shown in Fig. 2. Figure 2(a) shows the continuous mode data. This data format is applied to downstream data in PON systems. Figs. 2(b) and (c) show the burst mode data. Figure 2(b), which we call "isolated pattern", assumes low traffic. The response time of the B-Rx from a discharged state to a charged state is evaluated with this pattern. In Fig. 2(c), which we call "fulfilled pattern" with alternate power (maximum and minimum power with dynamic range), the signal amplitude may vary from packet to packet. The response time of the B-Rx from a maximum power burst to a minimum power burst is evaluated with this pattern. These patterns are used properly according to what has become one of the worst-case response time depending on the B-Rx design architecture.

The basic components of the optical receiver are a photodiode (PD), a trans-impedance amplifier (TIA) and a limiting amplifier (LA) as shown Fig. 3(a). When the average optical power of the input signal changes instantaneously, the degradation factors of the receiver response time are response speeds of the coupling interface and the control circuits, as the automatic gain control (AGC) and the automatic offset compensation (AOC) circuits. First, the optimal arrangement of these circuits in each amplifier should be considered.

In the continuous-mode optical receiver, the ac-coupling is usually used to connect different dc level of the receiver components and to save the power dissipation. The coupling capacitance depends on the length of the CID in the non-return-to-zero data format. If the signal includes long CIDs, the time constant of the ac-coupling differential interface becomes very long and the response speed is significantly degraded. To overcome this problem, dc-coupling has been used for B-Rx. Figure 3(b) shows the conventional dc-coupled B-Rx. When the SiGe ICs are adopted for the 10-Gbit/s-class optical receiver, the bias voltages of the ICs are usually positive. If a dc-coupled differential (positive logic) interface as shown in Fig. 3(b) is adopted, the bias voltages of the ICs must be the same. Consequently, the bias voltage of the TIA adjusts to that of LA and a linear dynamic range narrows. So, the AGC function is necessary for the TIA to ensure the sufficient dynamic range. The merit of employing AGC in TIA is to achieve the high speed response of the AOC in LA, because the input dynamic range of the LA can be narrow. Then, the response speed of this circuit depends only on the control circuits (AGC and AOC) in TIA. To shorten the response time, a peak-detect-and-hold circuit is adopted for dc-coupled B-Rx [10]. However, the optimal reset timing for the hold circuit depends on the turn-on characteristics of the B-Tx in each ONU, and this makes it difficult to guarantee the interoperability of the system. Moreover, this circuit design complicates because the threshold detection of the AOC must execute after the AGC operation in the TIA. Therefore, the response time of this B-Rx should be measured by the "isolated pattern" as shown in Fig. 2(b) with the strong burst signal whose power exceeds the threshold of the AGC.

Now let's change our mind and assume that the response speed of the ac-coupling interface can be sufficiently high, the bias voltage of the TIA can be set independently and the AGC can be omitted. Then, the response speed of B-Rx becomes just a response speed of the AOC circuits. In the ac-coupled B-Rx, the average detectors (ADs) are used as the threshold detector of the AOC as shown in Fig. 3(c) [11], [12]. They can continuously detect the threshold level without a reset signal and guarantee the interoperability. The response time of the AOC becomes time constant of the AD when the data format like the "isolated pattern" is input. However, the response time may be degraded when the data format like the "fulfilled pattern" is input according to the ratio of the maximum-power and the minimum-power burst signals. So, the worst-case response time of the ac-coupled one should be measured by the burst data format of the "fulfilled pattern".

Table 1 summarizes the differences between two types of B-Rx. The design concept of the dc-coupled B-Rx is based on the exclusion of the capacitive elements to eliminate transient phenomena. Therefore, the dc-coupled B-Rx can respond quickly, but it loses flexibility as regards the turn-on characteristics of the B-Tx, a simple interface, and a yield of fabrication. The design concept of the ac-coupled B-Rx is based on continuous mode Rxs that can obtain flex-

Table 1 Comparison of conventional B-Rxs.

Receiver type	Dc-coupled B-Rx	Ac-coupled B-Rx
Signal coupling	dc-couple	ac-couple
Threshold detection	Peak detect and hold type	Average detect type
Receiver settling time	ns	Mid or Late sub-μs
Reset signal (Interoperability)	Required	Not required
Fabrication yield	Low	High
Measured patterns	"Isolated pattern"	"Fulfilled pattern"

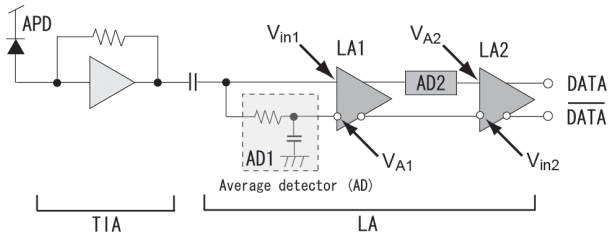

Fig. 4 Schematic diagram of our ac-coupled B-Rx.

ibility, simplicity and a high yield, but the response speed is slow compared with dc-coupled one because of the slow response of the ac-coupling interface and the average detectors of the AOCs. To overcome this problem, we have proposed a new design concept for the B-Rx based on ac-coupled architecture [13].

2.2 Configuration of Our B-Rx

Our design concept is based on the cancellation of the transient phenomena caused by the capacitive element that is put between TIA IC and LA IC by using counter phenomena. We proposed two design techniques, namely, the BLW-CMR technique and the inverted distortion technique. Our B-Rx is composed of an avalanche photodiode (APD) to obtain higher sensitivity, a single-ended TIA without an AGC function to eliminate the complexity of the circuit, two stage LAs (LA1 and LA2), and two ADs (AD1 and AD2) as shown in Fig. 4.

We describe the operation of our B-Rx using a time chart as shown in Fig. 5. The output voltage of the TIA is coupled with capacitors and branches to the differential input of LA1. Since AD1 is designed with a relatively small time constant, it operates instantaneously, and continuously detects the averages (threshold voltages: V_{A1}) of the signal as shown in Fig. 5(a). Then, V_{A1} follows the baseline-wander of the signal and it is cancelled by the common-mode rejection of LA1. This means that the response speed of this receiver depends solely on the time constant of the ADs. However, V_{A1} tends toward a high or low level for a long CID, which leads to duty-cycle distortion after the CIDs. LA2 and AD2 compensate for this distortion. The output voltage of AD2, namely V_{A2} is almost the same as V_{A1}, but the input signal of LA2, V_{in2}, is inverted as shown

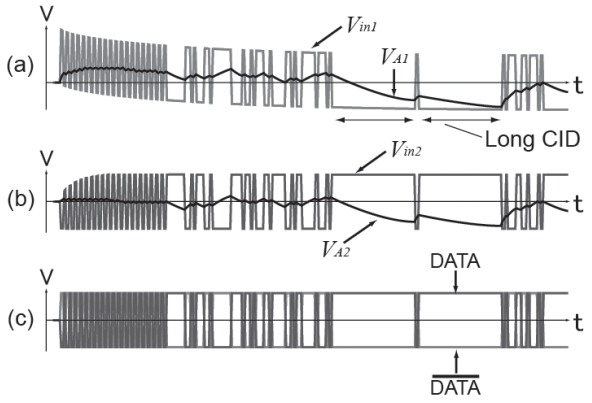

Fig. 5 Operating principle of ac-coupled B-Rx with BLW-CMR and inverted distortion techniques. (a) Input signal of LA1, (b) input signal of LA2, (c) output signal of LA2.

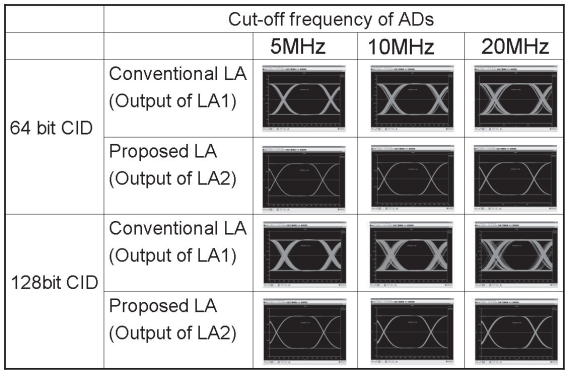

Fig. 6 Simulated eye patterns of our LA and conventional LA.

in Fig. 5 (b). The result is inverted distortion, which recovers the duty cycle as shown in Fig. 5(c). These techniques enable us to obtain both a quick response and high CID tolerance.

2.3 Analysis by Simulation of Our LA

We first simulated our LA to confirm the effectiveness of these techniques. In this simulation, we used the analog behavioral model on the HSPICE. The signal patterns consisted of an alternating "0" and "1" pattern as a preamble, and the payload data with a $2^{10} - 1$ pseudo random bit sequences (PRBS) that included 64- or 128-bit CIDs to evaluate a CID tolerance.

We evaluated the jitter peak-to-peak (J_{p-p}) when the cut-off frequency (f_{cl}) of the ADs was varied between 5 and 20 MHz. Figure 6 shows simulated eye patterns of our LA compared with that of a conventional LA consisting solely of AD1 and LA1. For a conventional LA, J_{p-p} deteriorated because duty cycle distortion was induced by long CIDs according to the increase in f_{cl}. On the other hand, we could confirm that the J_{p-p} of our LA became very low even if the f_{cl} increased. This result means that we achieved both the fast response and the high CID tolerance.

3. Experimental Results

3.1 Evaluation of Burst-Mode LA

The AD time constant is the key parameter to decide the response time and the CID tolerance. To clarify the optimum f_{cl} of the ADs using an empirical approach, we assembled our LA IC boards with various f_{cl} values (5, 10, and 20 MHz) for the ADs, and measured the electrical BER performance and the jitter degradation against each f_{cl}. Here, we used the electrical strong/weak burst data such as "fulfilled pattern" by the above-mentioned reason. Figure 7 shows an input burst signal pattern for evaluating the BER performance at a bit rate of 10.3 Gbit/s. Here, we used a 700 mV_{pp} electrical signal as the strong burst signal in consideration of the maximum TIA output. This pattern consisted of a preamble length of 800 ns applied to the burst mode synchronization pattern of the standardized IEEE 802.3 av (0x BF 40 18 E5 C5 49 BB 59), and a payload length of 1280 ns with a $2^{31} - 1$ PRBS [1]. The guard time was set at the 25.6 ns. The input voltage of the measured burst signal was varied between 10 and 150 mV_{pp}, namely, from −40 to −15 dBV. In addition, we defined the actual consumed preamble bits as the settling time of this LA IC.

Figures 8(a), (b), and (c) show the BER performance against each f_{cl} at preamble lengths of 800, 400, 200, 100, and 50 ns. The BER performance strongly depended on the preamble length because of the long AD time constant when f_{cl} was 5 MHz as shown in Fig. 8(a). This means that the response speed is too slow because of longer time constant of ADs. In contrast, for the f_{cl} of 20 MHz in Fig. 8(c), the preamble length was almost independent of the BER performance because the AD time constant was short. However, the BER performance at 20 MHz had deteriorated compared with that at 10 MHz, for instance at an input voltage of −33 dBV as shown by the circles in Figs. 8(b) and (c). This means that the reference voltage wandering was caused by the long CID, because the time constant of 20 MHz was too short.

After that, we measured J_{p-p} against f_{cl} for each input voltage (25, 30, 200, and 700 mV_{pp}). We used an input signal that included a 256-bit long CID in the payload data $2^{31}-1$ PRBS with a J_{p-p} of 0.13 UI to evaluate the CID tolerance. Figure 9 shows the J_{p-p} of the first bit after the 256-bit CID. The J_{p-p} value for f_{cl} values of 5, 10, and 20 MHz at an input voltage of 200 mV_{pp} were 0.188, 0.177, and 0.195 UI, respectively. These J_{p-p} values were sufficiently low compared with the 0.393 UI added at TP8 in IEEE 802.3 av [14]. We confirmed that the J_{p-p} at 20 MHz was degraded more by the long CID than those at 5 and 10 MHz. In contrast, the J_{p-p} with an f_{cl} of 10 MHz was the lowest in this experiment. So, we decided that the optimal f_{cl} for our LA IC was 10 MHz from the results shown in Figs. 8 and 9.

3.2 Optical Receiver Performance

Our B-Rx was composed of a commercial APD, a TIA, and our proposed LA. We fabricated our LA IC using a 0.18 μm SiGe BiCMOS process. The package size was $4 \times 4\,mm^2$. The power consumption was 0.15 W at +3.3 V for the bipolar circuit. The shunt capacitors of the AD are off-chip components to optimize the CID tolerance.

Figure 10 shows the experimental setup to confirm the

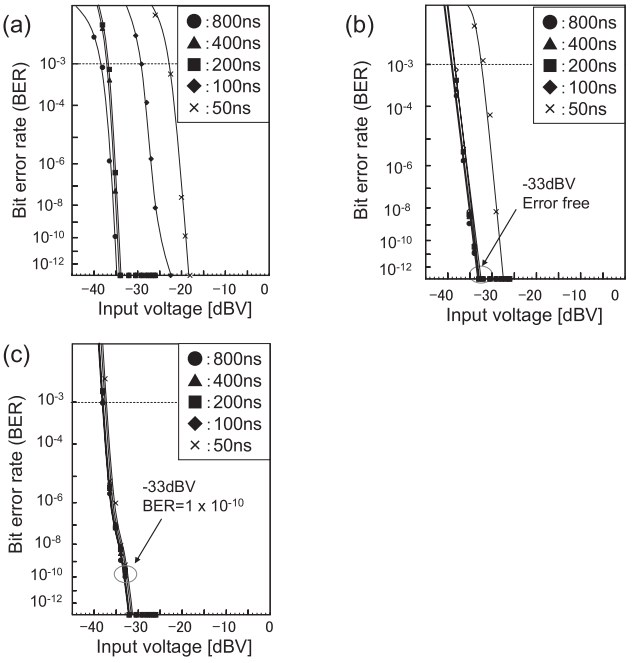

Fig. 8 Electrical BER performance against f_{cl} at preamble length 50, 100, 200, 400, 800 ns. (a) 5 MHz, (b) 10 MHz, (c) 20 MHz.

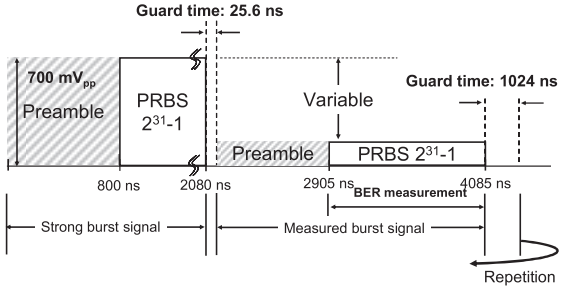

Fig. 7 Burst-signal pattern for electrical BER performance.

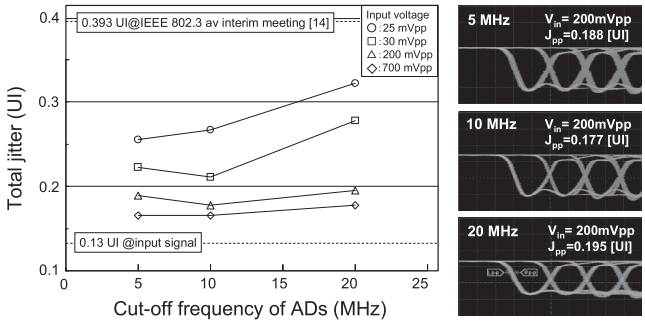

Fig. 9 Total jitter (J_{p-p}) against cut-off frequency (f_{cl}).

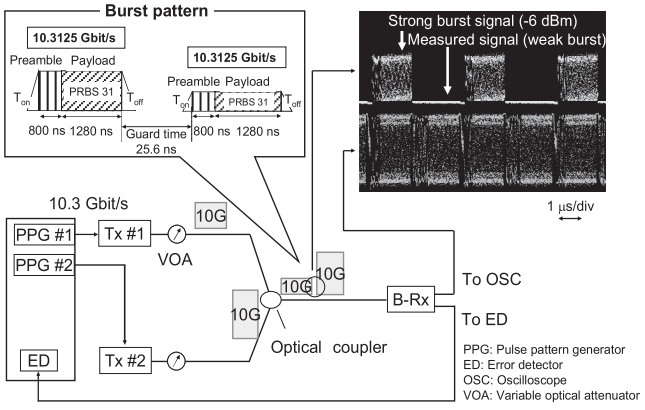

Fig. 10 Experimental setup. Inset: Waveforms for input optical signal, and output signal from our B-Rx.

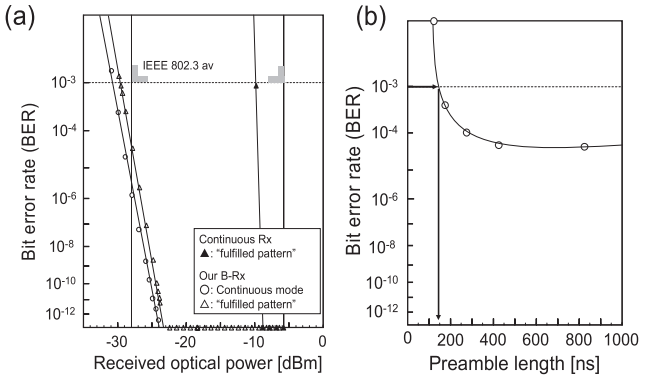

Fig. 11 (a): BER performance of our B-Rx. (b): Settling time of B-Rx.

BER performance and the settling times of our B-Rx. The B-Txs (Tx #1 and Tx #2) output 10.3-Gbit/s optical burst signals with extinction ratios of 6 dB including the $2^{31} - 1$ PRBS data [5]. These signals were input into a B-Rx consisting of a commercial APD-TIA and our LA whose f_{cl} was set at 10 MHz. The burst pattern was used to "fulfilled pattern" that is including the strong burst signal output from Tx #2 with an optical power of −6 dBm which is the maximum input power of IEEE 802.3 av.

Figure 11(a) shows the BER performance. Here, we also evaluated the BER characteristic of commercially available continuous mode Rx against the burst-mode data of "fulfilled pattern". The receiver sensitivity for continuous mode Rx was about −10 dBm when the BER was equal to 1×10^{-3} on assumption of the forward error correction (FEC). In contrast, the receiver sensitivity of our B-Rx was −29.8 dBm at a BER of 10^{-3}. The dynamic range of this B-Rx was 23.8 dB. The power penalty was only 0.2 dB between the continuous and burst mode data. Moreover, we estimated the minimum settling time of this receiver. We defined the actual consumed preamble bits as the settling time, and measured the minimum value under an ideal receiver sensitivity of −28 dBm standardized for PR30 of IEEE 802.3 av [1]. We confirmed that the receiver sensitivities for preamble lengths of 800, 400, 250, and 150 ns achieved IEEE PR30 (−28 dBm). Figure 11(b) shows an experimental result for the preamble length versus BER characteristics at an optical power of −28 dBm. This result indicates that the response time achieved 150 ns. This value is about one fifth that stipulated by the IEEE 802.3 av standardization.

4. Application of Burst-Mode Receiver

In this section, we describe several applications for B-Rxs in optical access networks.

(1): Dual-rate PON system

This system can provide existing and 10-Gbit/s class services on the same optical distribution network.

(2): Over 20 km transmission

Figure 11(a) shows that our B-Rx can secure a margin of 1.8 dB at a BER of 10^{-3} to meet the requirement of IEEE 802.3 av. We attempt to expand the PON system and achieve over 20 km transmission using this advantage.

4.1 Dual-Rate PON Systems

With a view to achieving smooth migration from 1G to 10G PON systems, it is desirable to realize a system in which they coexist. Such a system could provide existing services and new high bit rate services on the same optical distribution network, and so the capital expenditure needed to cover the cost of the fiber and the equipment for new services could be reduced. Therefore, the realization of coexisting systems is a major topic for discussion.

There are two kinds of dual rate PON systems. One is a coexisting system of the G- and NG-PON. This system can use a B-Rx corresponding to each bit rate by employing wavelength division multiplexing (WDM) technology being discussed at the Full Service Access Network (FSAN). The other is the 1G- and 10G-EPON system. These coexisting systems employ TDMA in the uplink because of the wavelengths of the overlap of 1G and 10G as shown in Fig. 12 [1], [15]. Therefore, a dual rate B-Rx for coexisting 1G- and 10G-EPON systems must be able to handle upstream traffic with significantly different optical powers, arbitrary phases, and dual bit rates. We have developed a dual rate B-Rx based on the above mentioned architecture.

Our dual-rate B-Rx is composed of an APD, a TIA, a 1G-LA, a 10G-LA, and two gate circuit (GCs) to eliminate the frequency instability of the CDR as shown in Fig. 13(a). Figure 13(b) shows waveforms input/output from a dual-rate B-Rx as shown in Fig. 13(a). "A" shows a mixed 1G- and 10G optical waveform. "B" shows the output waveform from the 10G-LA. "C" shows the external rate select signal to control the GCs. "D" shows the output waveform from the "10G output port" of the GC. "E" shows the output waveform from the "1G output port" of the GC. Here, each GC outputs a signal only when the rate select signal from the MAC-LSI is "HI". So, mixed 1G- and 10G-burst signals are separated only into "1G-signals" and "10G-signals".

Then, we evaluated the BER characteristics of this re-

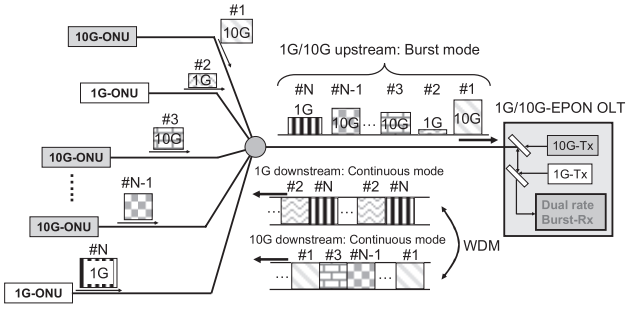

Fig. 12 Coexistence of 1G- and 10G-EPON systems.

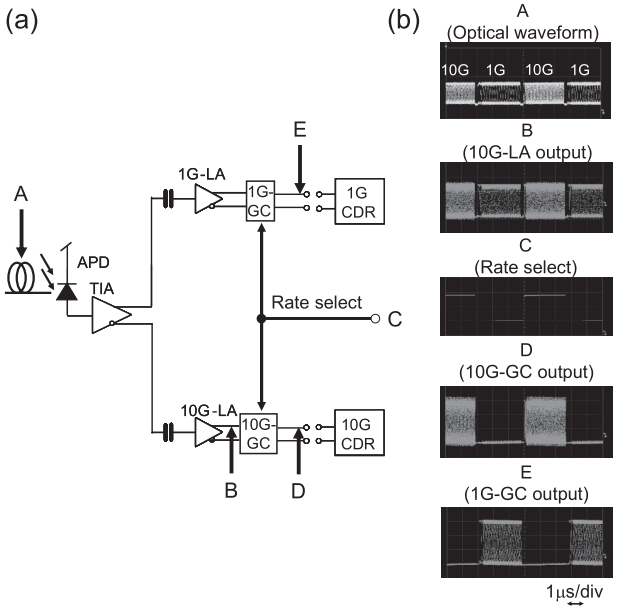

Fig. 13 (a): Configuration of dual-rate B-Rx. (b): Measured waveform.

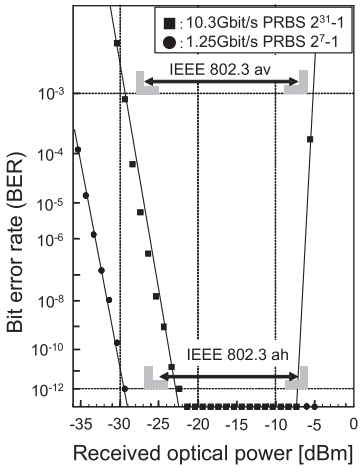

Fig. 14 BER characteristic of our dual-rate B-Rx.

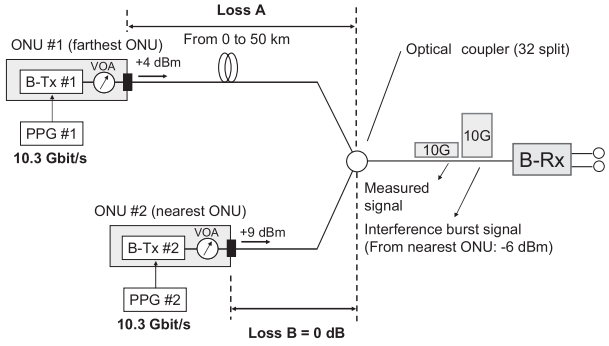

Fig. 15 Experimental setup over 20 km uplink transmission.

ceiver. To obtain this result, we used mixed strong/weak 1G- and 10G-signals to evaluate the effect of an input signal with different bit-rate. The burst-mode transmitters output 10.3- and 1.25-Gbit/s optical burst signals with extinction ratios of 6 dB including $2^{31}-1$ and 2^7-1 PRBS data, respectively. The optical powers of the signals were adjusted by using VOA, and the signals were input into our dual rate B-Rx as well as Sect. 3.3. Here the optical signal output from one of the burst-mode transmitter was an interference burst signal with an optical power of −6 dBm. The burst pattern had a preamble length of 800 ns, a payload length of 1280 ns, and a guard time of 25.6 ns. Figure 14 shows the BER characteristics of burst-mode signals at 10.3 and 1.25 Gbit/s output from the GCs. For the 1.25 Gbit/s signal, we achieved a receiver sensitivity of −29.3 dBm, an input overload of more than −5 dBm at a BER of 10^{-12}, and a dynamic range of over 24.3 dB. For the 10.3-Gbit/s signal, we realized a sensitivity of −29.5 dBm, an input overload of −5 dBm at a BER of 10^{-3}, and a dynamic range of 24.5 dB. These values satisfied the IEEE 802.3 ah and av standardization requirements.

4.2 Over 20 km Transmission

Improving the long reach of access systems will become increasingly important if we are to offer PON-based services to long-distance customers more effectively. To satisfy this requirement, long-reach PON systems using optical amplifiers are now being actively investigated [16], [17]. However, the electric power supply and the development of burst-mode optical amplifier are critical problems to achieve expansion of budget in PON systems. To this end, we attempted to expand the PON system to achieve transmission of over 20 km using this B-Rx without an optical amplifier.

Figure 15 shows the experimental setup we used for an uplink transmission of over 20 km. To emulate the worst case cited in the IEEE 802.3 av standardization, the transmission optical power from ONU #1, which is the farthest ONU with the minimum average launch power, was set at +4 dBm, and that from ONU #2, which is the nearest ONU with the maximum average launch power, was set at +9 dBm. An optical coupler with 32 branches was located between ONUs and OLT. We defined loss A as the transmission loss between ONU #1 and the optical coupler. On the other hand, the loss B, which we defined as the transmission loss between ONU #2 and the optical coupler, was

Table 2 Actual values of transmission loss, optical power at B-Rx, and dynamic range.

Transmission distance [km]	Loss A [dB]	Total loss [dB] (A + split loss)	Optical power at B-Rx [dBm]	D-range [dB]
0	0	16.8	-12.8	6.8
10	3.96	20.76	-16.76	10.76
20	6.86	23.66	-19.66	13.66
30	10.82	27.62	-23.62	17.62
40	13.77	30.57	-26.57	20.57
50	17.73	34.1	-30.1	24.1

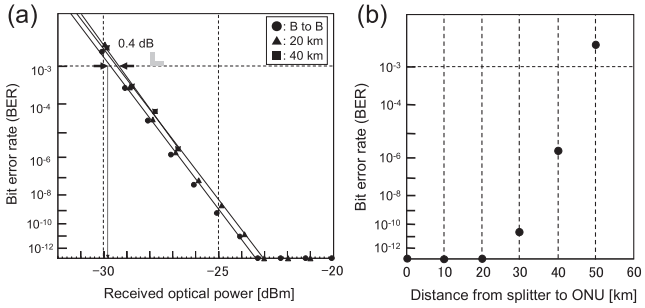

Fig. 16 (a): BER performance for 20 and 40 km transmission. (b): Distance from splitter to ONU versus BER.

almost 0 dB. Table 2 shows the actual values of the transmission loss, the optical power at B-Rx, and the dynamic range. Here, the optical input power to a B-Rx of ONU #2 (nearest ONU) was adjusted to become −6 dBm in consideration of the excess loss of the optical coupler. For a 40 km transmission, loss A, input optical power, and dynamic range between ONU #1 and ONU #2 were 13.77 dB, −26.57 dBm, and 20.57 dB, respectively. In addition, the burst pattern and the guard time were set up on the same condition as Sect. 3.3.

Figure 16(a) shows the BER characteristics for each transmission distance. The closed circles, triangles, and squares correspond to transmission distances of 0, 20 and 40 km, respectively. From the results of Fig. 11(a) and Table 2, the BER of the 50 km transmission exceeded the FEC limit (BER = 1×10^{-3}). The power penalty for transmission between 0 and 40 km transmissions was only 0.4 dB. Figure 16(b) shows an experimental result for the transmission distance versus BER characteristic. 40 km PON systems can be achieved by using our B-Rx with FEC.

5. Conclusion

An average-detection-type B-Rx was demonstrated based on ac-coupled architecture for 10-Gbit/s class PON systems by using BLW-CMR and inverted distortion techniques. Our B-Rx can realize a high sensitivity, a wide dynamic range, and an instantaneous response with a high CID tolerance. In experiments, we achieved receiver sensitivities of −29.8 dBm at a BER of 10^{-3} with a strong/weak burst data. The settling time of our B-Rx was less than 150 ns. This is the fastest value for any reported ac-coupled average-detection type burst-mode receiver at a $2^{31} - 1$ PRBS.

Moreover, we also described several potential applications of the B-Rx, namely, a dual rate PON system and a transmission experiment of over 20 km. When we employed our B-Rx, the proposed systems achieved better performance. This circuit design and these results will contribute to the realization of more flexible future broadband optical access networks.

References

[1] IEEE P802.3av, http://www.ieee802.org/3/av/
[2] J. Kani, F. Bourgart, A. Cui, A. Rafel, M, Campbell, R. Davey, and S. Rodrigues, "Next-generation PON Part I: Technology roadmap and general requirements," IEEE Commun. Mag., vol.47, no.11, pp.43–49, 2009.
[3] D. Breuer, R. Hülsermann, C. Lange, T. Monath, and E. Weis, "Architectural options and challenges for next generation optical access," Proc. ECOC 2010, Mo.2.B.1, 2010.
[4] S. Yoshima, M. Nogami, S. Shirai, N. Suzuki, M. Noda, H. Ichibangase, and J. Nakagawa, "A 10.3 Gbit/s LAN-PHY based burst-mode transmitter with a fast 6 ns tur n-on/off time for 10 Gbps-based PON systems," Proc. OFC/NFOEC 2008, OWL4, 2008.
[5] H. Nakamura, S. Kimura, K. Hara, N. Yoshimoto, M. Tsubokawa, M. Nakamura, K. Nishimura, A. Okada, and Y. Ohtomo, "AC-coupled burst-mode transmitter using baseline-wander common-mode-rejection technique for 10-Gbit/s-class PON systems," J. Lightwave Technol., vol.27, no.3, pp.336–342, 2009.
[6] Y. Lin, E. Zhu, and G. Gu, "A 10 Gb/s burst-mode laser diode driver for IEEE 802.3av 10G-EPON applications," Proc. 2010 Second International Conference on Future Networks, pp.256–260, 2010.
[7] J. Nakagawa, M. Nogami, N. Suzuki, M. Noda, S. Yoshima, and H. Tagami, "10.3-Gb/s Burst-Mode 3R Receiver Incorporating Full AGC Optical Receiver and 82.5-GS/s Over-Sampling CDR for 10G-EPON Systems," IEEE Photonics Technol. Lett., vol.22, no.7, pp.471–473, 2010.
[8] X.Z. Qiu, C. Melange, T. De Ridder, B. Baekelandt, J. Bauwelinck, X. Yin, and J. Vandewege, "Evolution of burst mode receivers," Proc. ECOC 2009, 7.5.1, 2009.
[9] S. Nishihara, S. Kimura, T. Yoshida, M. Nakamura, J. Terada, K. Nishimura, K. Kishine, K. Kato, Y. Ohtomo, N. Yoshimoto, T. Imai, and M. Tsubokawa, "A burst-mode 3R receiver for 10-Gbit/s PON systems with high sensitivity, wide dynamic range, and fast response," J. Lightwave Technol., vol.26, no.1, pp.99–107, 2008.
[10] P. Ossieur, D. Verhulst, Y. Martens, W. Chen, J. Bauwelinck, X.Z. Qiu, and J. Vandewege, "A 1.25-Gb/s burst-mode receiver for GPON applications," IEEE J. Solid-State Circuits, vol.40, no.5, pp.1180–1189, 2005.
[11] J. Wook Kwon, J. Lee, J. Baek, J. Cho, J. Seo, S. Park, J. Lee, Y. Oh, and D. Jang, "AC-coupled burst-mode OLT SFP transceiver for Gigabit Ethernet PON systems," IEEE Photonics Technol. Lett., vol.17, no.7, pp.1519–1521, 2005.
[12] S. Han and M.S. Lee, "Transmission performance of AC-coupled burst-mode optical receiver for Ethernet PON," Advanced Communication Technology, vol.1, pp.450–453, 2004.
[13] S. Kimura, "10-Gbit/s TDM-PON and over-40-Gbit/s WDM/TDM-PON systems with OPEX-effective burst-mode technologies," Proc. OFC/NFOEC 2009, OWH6, 2009.
[14] IEEE P802.3av TF, IEEE 802.3 Interim Meeting, Seoul, South Korea, Sept. 2008
[15] IEEE P802.3ah TF, http://www.ieee802.org/3/ah/
[16] J. Bauwelinck, B. Schrenk, F. Bonada, B. Baekelandt, J. Lazaro, P. Chanclou, J. Prat, and X.Z. Qiu, "Full-duplex 10 Gb/s transmission in ultra-dense PONs with tree splits > 1:1k and noise-powered extender box," Proc. ECOC 2010, Tu.5.B.4., 2010.

[17] M. Fujiwara, K. Suzuki, K. Hara, T. Imai, K. Taguchi, H. Ishii, N. Yoshimoto, and H. Hadama, "Burst-mode compound optical amplifier with automatic level control circuit that offers enhanced setting flexibility in a 10 Gb/s-Class PON," Proc. ECOC 2010, PD3_3, 2010.

Kazutaka Hara received B.E., and M.E. degrees in applied physics from Tokyo University of Science and Tokyo Institute of University, Japan in 2003 and, 2005, respectively. In 2005, he joined NTT Access Network Service Systems Laboratories, where he engaged in research on optical transmission systems. Since 2007 he has been in charge of research on 10 Gigabit-class high-speed TDM access systems. He is a member of the Institute of Electronics, Information, and Communication Engineers (IEICE) of Japan. He was the recipient of the Best Paper Award at the OptoElectronics and Communications Conference (OECC) 2010 and at the International Conference on Optical Internet (COIN) 2010.

Shunji Kimura received B.E. and M.E. degrees in electrical engineering in 1989 and 1991, respectively and a Ph.D. in electronics, information and communication engineering in 1997, all from Waseda University, Tokyo, Japan. In 1991, he joined Nippon Telegraph and Telephone Corporation (NTT) LSI Laboratories, where he engaged in design and evaluation technologies related to MMICs for high-speed optical transmission systems. He is currently with NTT Access Network Service Systems Laboratories, Yokosuka, Kanagawa, Japan, where he is working on the development on the broadband optical access network systems and the optical video delivery systems. Dr. Kimura is a member of the IEEE. He was the recipient of the 1994 Japan Microwave Prize presented at the Asia-Pacific Microwave Conference and the 1996 Young Engineer Award from the IEICE of Japan.

Hirotaka Nakamura received B.E. degree in applied physics from the University of Tokyo, Tokyo, Japan, in 1999. In 1999, he joined NTT Access Network Service Systems Laboratories, Japan, and was engaged in research on optical access systems using wavelength-division-multiplexing (WDM) technologies. He is currently working on 10 Gigabit-class PON systems and next generation PON systems.

Naoto Yoshimoto is R&D Manager at NTT Laboratories. He received B.S., M.S., and Ph.D. degrees in electronics and information engineering from Hokkaido University, Japan, in 1986, 1988, and 2003, respectively. He joined NTT Laboratories in 1988, and engaged in the research and development of optical transmission equipment and related optical modules for broadband access systems. He is currently a senior manager of NTT Access Network Service Systems Laboratories, and is engaged in the planning and design of next-generation optical access network services and architectures mainly based on high-speed TDM-PON and cost-effective WDM technologies. In particular, he has recently been focusing on technology as regards 10G-EPON systems. Dr. Yoshimoto is a member of the IEEE Communication Society. He is also a member of the technical program committee of the European Conference on Optical Communication (ECOC) during 2006–2007 and the Optical Fiber Communication (OFC) during 2009–2011. He was the recipient of the 1994 Young Engineer Award from the IEICE of Japan.

Hisaya Hadama received B.S. and M.S. degrees from Kyushu University, and a D. Eng. degree from Osaka University in 1985, 1987, and 1997, respectively. After he joined NTT in 1987, he engaged in the research of ATM Virtual Path transport networks. During 1994–1995 he worked for research of multimedia network control techniques, as a visiting researcher at Center for Telecommunications Research, Columbia University. After returning to Japan, he engaged in NTT's R&D strategy of Global Mega-media Network, which aimed to realizing affordable broadband network access services. During 2003–2009, he worked for research for ubiquitous network service systems, the Wide Area Ubiquitous Network Systems, and an architectural design of New Generation Network of NTT. He completed Executive MOT program of MIT Sloan School in 2005. He is currently a Project Manager of Optical Access Systems Project in the NTT Access Network Service Systems Laboratories. He is a member of IPSJ and IEEE.